Journal of the Korean Geo-Environmental Society
19(2): 13~21. (February 2018) http://www.kges.or.kr
ISSN 1598-0820
DOI https://doi.org/10.14481/jkges.2018.19.2.13

Effect of the Permeability of Excavation Wall on the Earth Pressure in a Jointed Rock Mass

Moorak Son† · Solomon Adedokun[1)]

Received: October 31st, 2017; Revised: November 10th, 2017; Accepted: January 29th, 2018

ABSTRACT : The magnitude and distribution of earth pressure on the excavation wall in jointed rock mass were examined by considering different wall permeability conditions as well as rock types and joint inclination angles. The study was numerically extended based on a physical model test (Son & Park, 2014), considering rock-structure interactions with the discrete element method, which can consider various characteristics of rock joints. This study focused on the effect of the permeability condition of excavation wall on the earth pressure in jointed rock masses under a groundwater condition, which is important but has not been studied previously. The study results showed that the earth pressure was highly influenced by wall permeability as well as rock type and joint condition. Earth pressure resulted from the study was also compared with Peck's earth pressure in soil ground, and the comparison clearly showed that the earth pressure in jointed rock mass can be greatly different from that in soil ground.

Keywords : Rock excavation, Earth pressure, Wall permeability, Rock type, Joint inclination angle, Rock-structure interaction

1. Introduction

Deep excavation in congested urban areas is increasing due to construction of new buildings and development of infrastructures. However, the effect of excavation works on the surrounding environment is also increasing and has become a major concern. To reduced excavation-related problems such as an impact on surrounding area or wall collapse, a clear understanding on the behavioral characteristics of the ground and excavation wall is necessary.

Many researchers have studied of the earth pressure on the excavation walls by through field measurements and physical model tests. Among them, Peck (1969) & Tschebotarioff (1973) suggested the apparent earth pressure envelopes (Fig. 1) for soil ground, which are frequently used in the field for designing excavation walls in soil ground. However, most existing studies were for soil grounds though the ground is made up of not only soils but also rocks. It is unclear whether their findings for soil grounds can be extended to rock strata or not. Some field measurements (Chae & Moon, 1994; Jeong & Kim, 1997; Yoo & Kim, 2000) were also carried out in multi-layered ground including rocks, but their studies only focused on the comparison of the measured earth pressure magnitude with Peck's earth pressure without any consideration of joint conditions. Nevertheless, it was hard to find the studies that have examined the earth pressure on support systems in rock strata with systematic rock and joint conditions until recently. More systematic studies on the earth pressure in jointed rock masses have been carried out in the recent years by Son (2013), Son & Park (2014), Son et al. (2015), considering rock type, joint condition (joint inclination angle and joint shear strength), and support conditions. The study results clearly indicated that the earth pressure in jointed rock masses can be significantly different in soil and rock grounds, depending on rock type, joint condition, and support condition.

This study extended the previous studies further, focusing on the effect of the permeability of excavation wall on the earth pressure in jointed rock masses under a groundwater condition, which is important but has not been studied previously. Numerical parametric studies were conducted by varying wall permeability as well as rock type and joint condition. The results from this study are expected to provide a better understanding of the earth pressure on the excavation wall in jointed rock masses.

† Department of Civil Engineering, Daegu University (Corresponding Author : mson@daegu.ac.kr)
1) Department of Civil Engineering, Daegu University

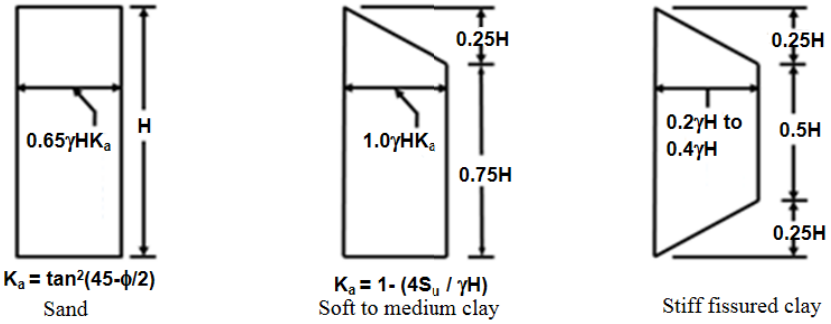

(a) Apparent earth pressure (Peck, 1969)

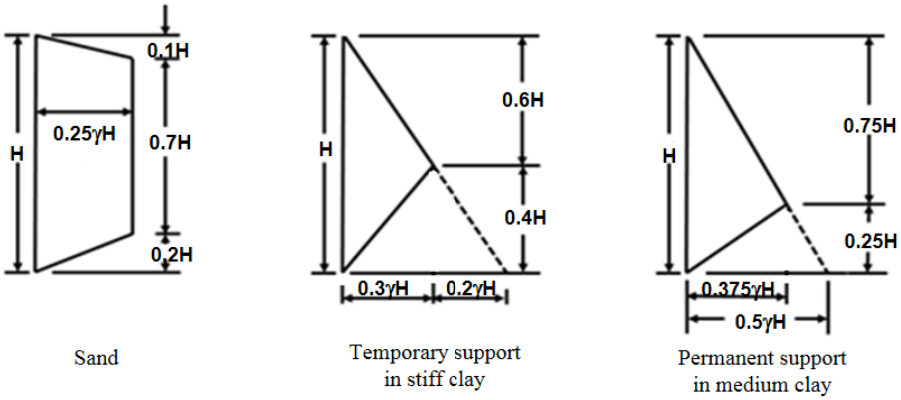

(b) Apparent earth pressure (Tschebotarioff, 1973)

Fig. 1. Apparent earth pressure for soils

2. Numerical approach and extended parametric study

In this study, the numerical approach is similar to the previous study (Son & Park, 2014), and a brief description is followed as below. The numerical approach was previously verified by the comparison between a physical model test and its numerical simulation (Figs. 2 and 3). The controlled parameters in the study includes the wall permeability and groundwater conditions (wall under no groundwater, permeable wall under groundwater, impermeable wall under groundwater) as well as rock types and joint conditions. Table 1 summarizes the considered conditions in this study. The groundwater table was assumed to be at the ground surface.

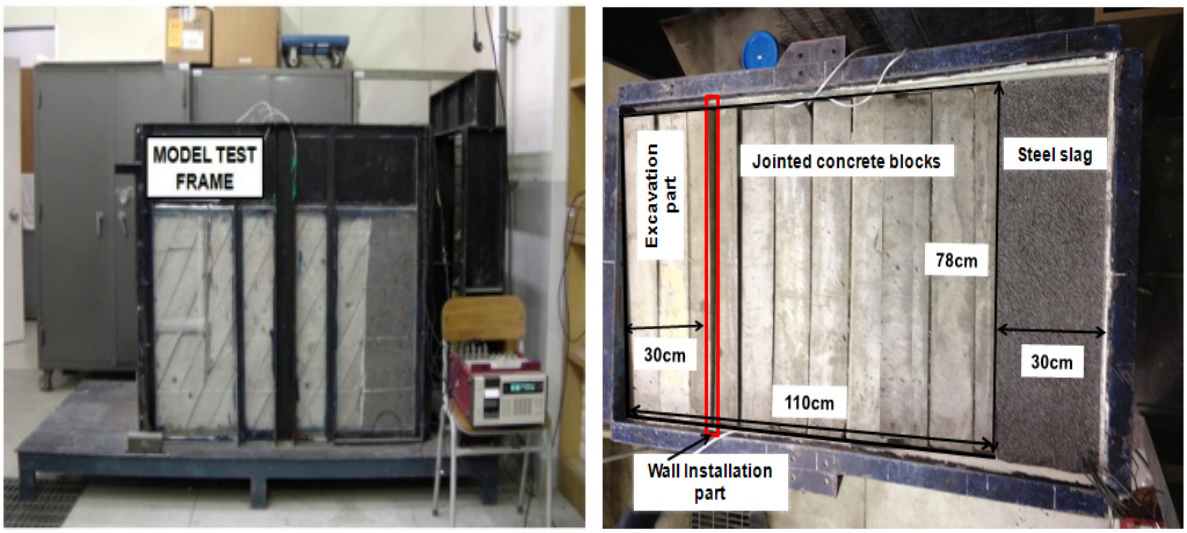

Fig. 2. Test preparation for physical model (Son & Park, 2014)

This study used 2-D Universal Distinct Element Code (UDEC, 2004), which allows for large displacements between rock blocks. Elastic elements were considered for the rock blocks, wall and struts and the joints between the rock blocks and the interfaces between walls and rocks were modeled using the Coulomb slip model. A fully coupled mechanical-hydraulic analysis was performed, in which joint porewater pressures affected the mechanical computations. The coupled behavior was examined using the method of fluid flow in joints provided by the DEM code.

The considered model was 68.8 m x 31.5 m and the excavation wall was installed at the depth of 20.5 m (Fig. 4). The excavation width was assumed to be 20 m and the final excavation depth was 19 m. A strut-supported system

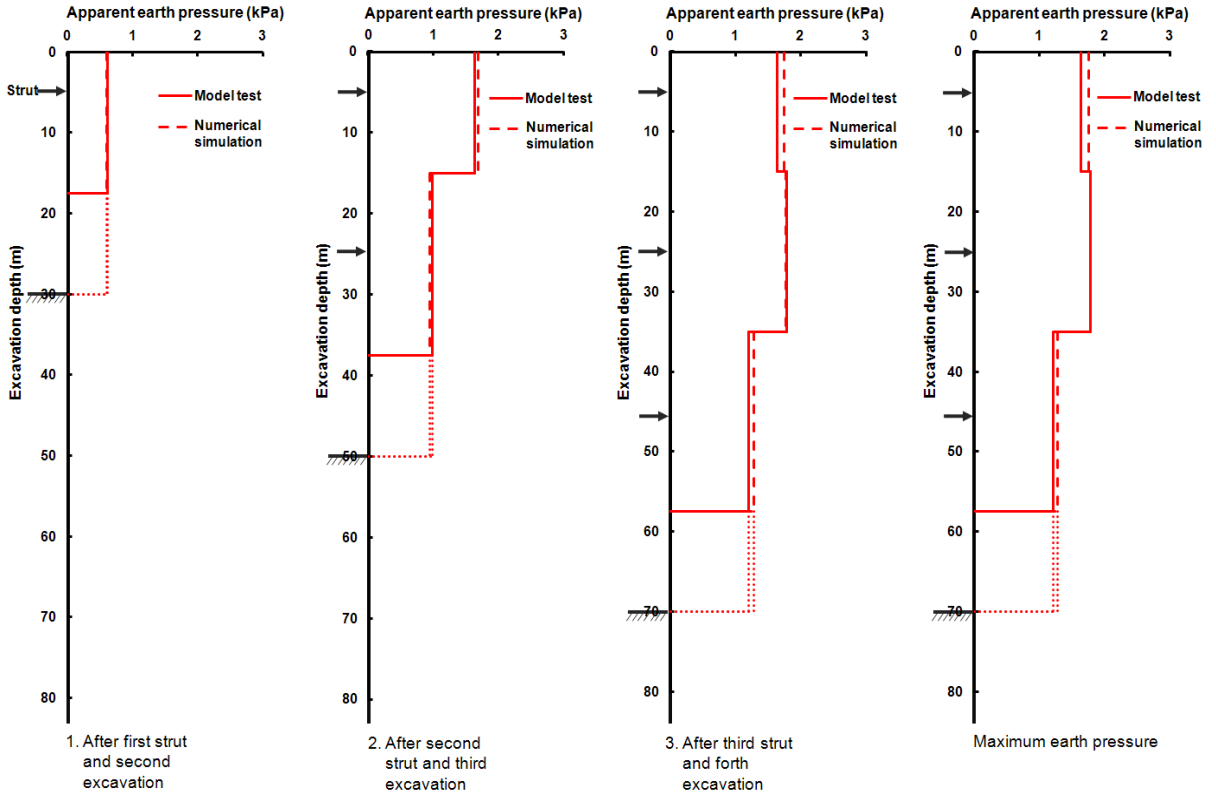

Fig. 3. Comparison between physical model test and numerical simulation (Son & Park, 2014)

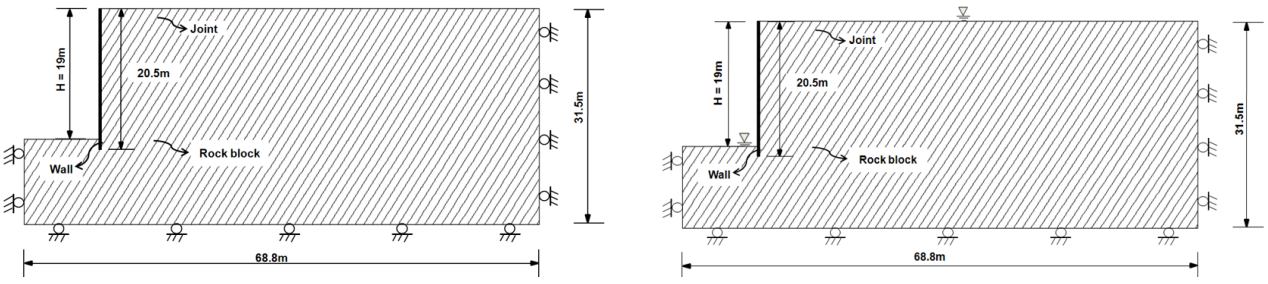

(a) No groundwater condition (b) Groundwater condition

Fig. 4. Numerical modeling (a case of joint inclination angle of 60°)

Table 1. Controlled parameters for numerical analyses

Parameters / Rock type	Wall permeability condition	Joint inclination angle (°)	Joint shear condition	Earth pressure coefficient
Hard	NG[1], GWPW[2], GWIW[3]	30, 90	Good	1
Moderately weathered	NG[1], GWPW[2], GWIW[3]	30, 90	Poor	1

1): No groundwater, 2): Groundwater with permeable wall, 3): Groundwater with impermeable wall

was used because the empirical earth pressure (Peck, 1969), which was compared with this study's results, was also obtained from many sets of comprehensive measurements of the strut load in strut-supported excavation walls.

The joint inclination angle was measured in the anticlockwise direction from the horizontal plane, and the in-situ earth pressure coefficient and joint spacing was assumed to be 1.0 and 1 m respectively. The analysis was carried out using H- pile and timber lagging wall. In order to reflect the general excavation procedures in the field, eight excavation stages were conducted to obtain the distribution and magnitude of earth pressure. Before the first excavation was carried out, the initial equilibrium was obtained with the at-rest earth pressure coefficient. At this stage, the boundary condition was a roller at each end of the two vertical boundaries and at the bottom boundary. After ensuring the initial equilibrium condition, all displacements were reset to zero and the wall was installed at a depth of 20.5 m. The first excavation was conducted up to 1.0 m, followed by the installation of the first strut at 0.5 m over the excavation line. After the first excavation, there was additional excavation work every 3 m, which was followed by the strut installation at every 3 m interval (which is 0.5 m above each excavation line). Wall stabilization was ensured after each excavation stage. The final excavation was conducted up to 19.0 m, and no strut was installed in the final stage (see Fig. 5). Other analyses were also carried out for different groundwater conditions and earth pressure coefficients using the same procedures discussed above.

The shape of typical excavation wall (i.e. H-pile and timber lagging wall) might have little effect on the earth pressure and wall displacement in the field as long as the flexural stiffness of the wall is equivalent. However, in a numerical analysis the shape may have a considerable influence on the results because of a stress concentration in modeling. To address this issue, this study transformed the excavation wall into a simple section to represent the equivalent flexural stiffness of the wall (see Fig. 6). The properties of the wall, rocks, joints, and interfaces used in numerical analysis are shown in Table 2. The properties were determined based on Hoek & Brown (1988), Goodman (1989), and Bieniawski (1989). Bieniawski's method was used to compute the rock mass rating (RMR) for hard rock with good joint conditions and 1-m joint spacing. The rock mass elastic modulus E_m

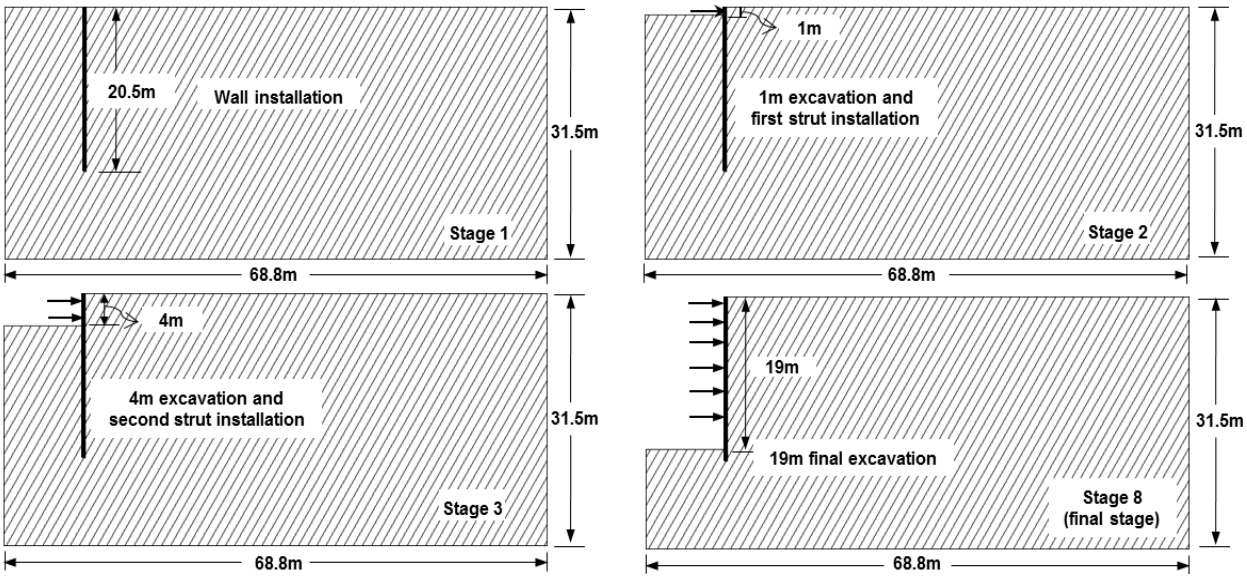

Fig. 5. Excavation stages in numerical modeling (a case of joint inclination angle of 60°)

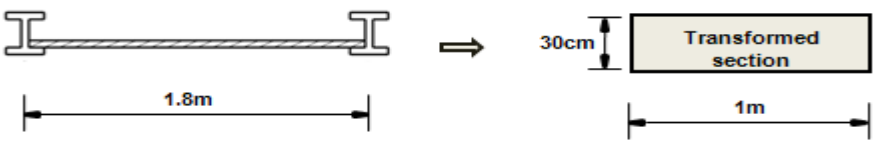

Fig. 6. Transformed section in numerical modeling

Table 2. Properties of the wall, rocks, joints and interfaces used in the analysis

Rock type	Wall	Rock and joint												Rock-Wall interface			
		Rock			Joint												
	EI ($MPa.m^4$)	E_r (MPa)	υ	γ_r (MN/m^3)	Joint condition	c,σ_t (MPa)	ϕ (°)	ϕ_r (°)	k_n (MPa/m)	k_s (MPa/m)	a (m)	a_{res} (m)	μ (Pa.sec)	c,σ_t (MPa)	δ (°)	k_s (MPa/m)	k_s (MPa/m)
Hard	23.20	1.0×10^5	0.2	2.7×10^{-2}	Good	0	50	35	2.33×10^5	0.96×10^5	3×10^{-4}	2×10^{-4}	10^{-3}	0	33	2.33×10^5	0.96×10^5
Moderately weathered		1.0×10^3	0.25	2.5×10^{-2}	Poor	0	35	31.5	2.33×10^3	0.96×10^3	3×10^{-4}	2×10^{-4}	10^{-3}	0	23	2.33×10^3	0.96×10^3

EI = Wall bending stiffness; E_r = Intact rock elastic modulus; υ = Poisson's ratio; γ_r = Unit weight of intact rock; c = Joint or interface cohesion; σ_t =Joint or interface tensile strength; ϕ = Joint friction angle; ϕ_r = Joint residual friction angle; δ = Interface friction angle; k_n = Joint or interface normal stiffness; k_s = Joint or interface shear stiffness; a = Joint aperture; a_{res} = Joint residual aperture; μ = Dynamic viscosity of water

was then determined from the equation E_m = 2RMR-100 proposed by Bieniawski. This value was used to calculate the joint normal and shear stiffness for the numerical parametric studies as follows:

$$\text{Joint normal stiffness: } k_n = \frac{E_m E_r}{S(E_r - E_m)}$$

$$\text{Joint shear stiffness: } k_s = \frac{G_m G_r}{S(G_r - G_m)}$$

where E_m is the shear modulus of the rock mass, G_m is the shear modulus of the rock mass, E_r is the elastic modulus of intact rock, G_r is the shear modulus of intact rock, and s is the joint spacing.

The rock mass elastic modulus for slightly and moderately weathered rocks was determined by reducing the rock mass elastic modulus for hard rock by factors of 10 and 100, respectively. The joint normal and shear stiffness of these rocks were then calculated using the same procedures discussed above. Son & Yoon (2011) explained in detail of the assessment of the properties.

The strut axial stiffness used for the numerical simulation was determined as follows:

$$\text{Strut axial stiffness, } k_{sup} = \frac{EA}{L \times Space}\cos\theta$$

where A is the section area of a strut (300 x 300 x 10 x 15 mm, H-section), E is the strut elastic modulus, L is half of the strut length, *Space* is the horizontal strut spacing, and q is the installation angle of the strut (zero for horizontal installation).

3. Effect of the permeability of excavation wall under different rock conditions

Figs. 7 and 8 compare the distributions of the apparent earth pressures induced on the excavation walls for hard rock at the joint inclination angles of 30° and 90° respectively under different wall permeability and groundwater conditions. In the figures, the induced earth pressures were represented in terms of apparent earth pressures in which the magnitude and distribution of earth pressures on the excavation wall were inferred from the strut axial loads in the same way as Peck (1969). In addition, the induced apparent earth pressures in jointed rock masses were compared with Peck's apparent earth pressure suggested for sand ground with a friction angle of ϕ = 35°. The apparent earth pressure ratio represents the ratio of the induced earth pressure for jointed rock mass to Peck's earth pressure for the sand ground. Fig. 9 compares the total earth pressure ratios (the area of an induced apparent earth pressure distribution envelope divided by the area of Peck's apparent earth pressure envelope) of the induced earth pressures from numerical analysis with that from Peck's empirical earth pressure for the sand ground.

For a joint inclination angle of 30°, the total earth pressure ratio was 0.033 under no groundwater condition. The earth pressure with a permeable wall under groundwater was similar to that of the no ground water condition (see Figs. 7 and 9). However, the earth pressure with an impermeable wall under groundwater increased and the earth pressure ratio was 0.53. The increase can be attributed to the decrease in joint shear strength due to the induced pore water pressure.

For a joint inclination angle of 90°, the apparent earth pressures of the no groundwater condition were similar to

those of a joint inclination angle of 30°. The total earth pressure ratio was 0.035. However, the earth pressure with a permeable wall under groundwater was very different from that of the no ground water condition and the total earth pressure ratio was 0.68. It was rather similar to that with an impermeable wall in which the total earth pressure ratio was 0.68 (see Fig. 9). The reason can be attributed to the fact that the impermeable rock blocks with vertical joints acted like an impermeable excavation wall.

Figs. 10 and 11 compare the distributions of the apparent earth pressures induced on the excavation walls for moderately weathered rock at the joint inclination angles of 30° and 90°

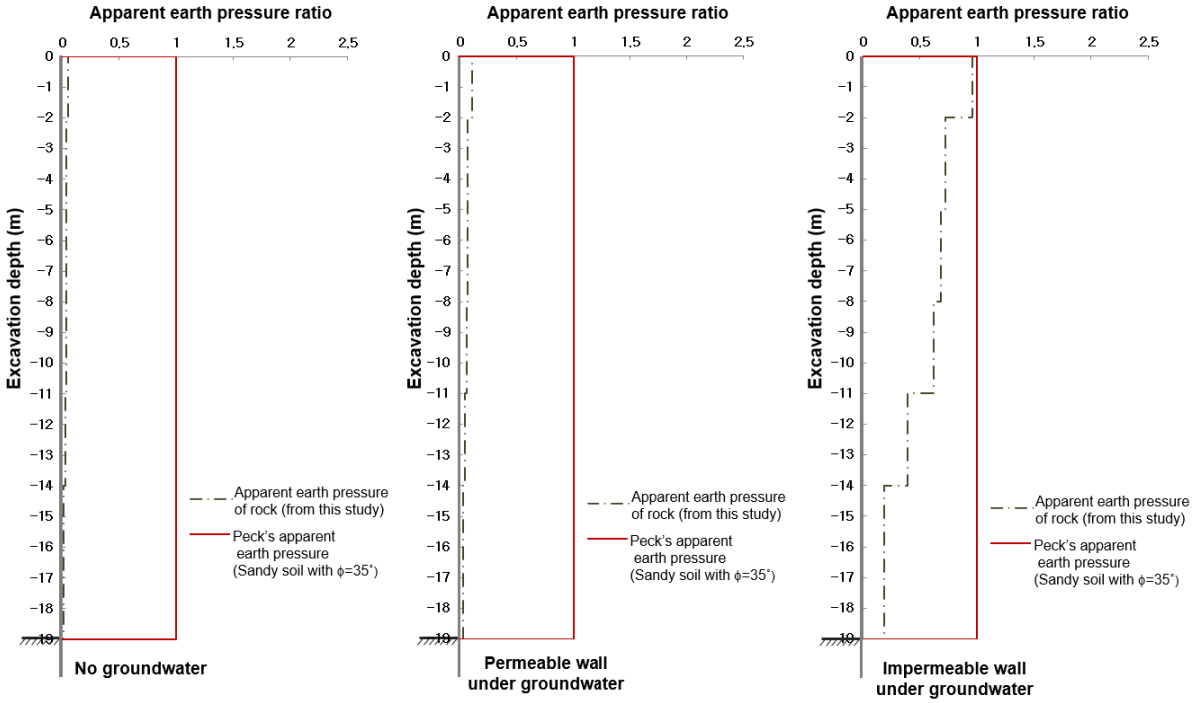

Fig. 7. Comparison of the apparent earth pressures for hard rock (joint inclination angle: 30°)

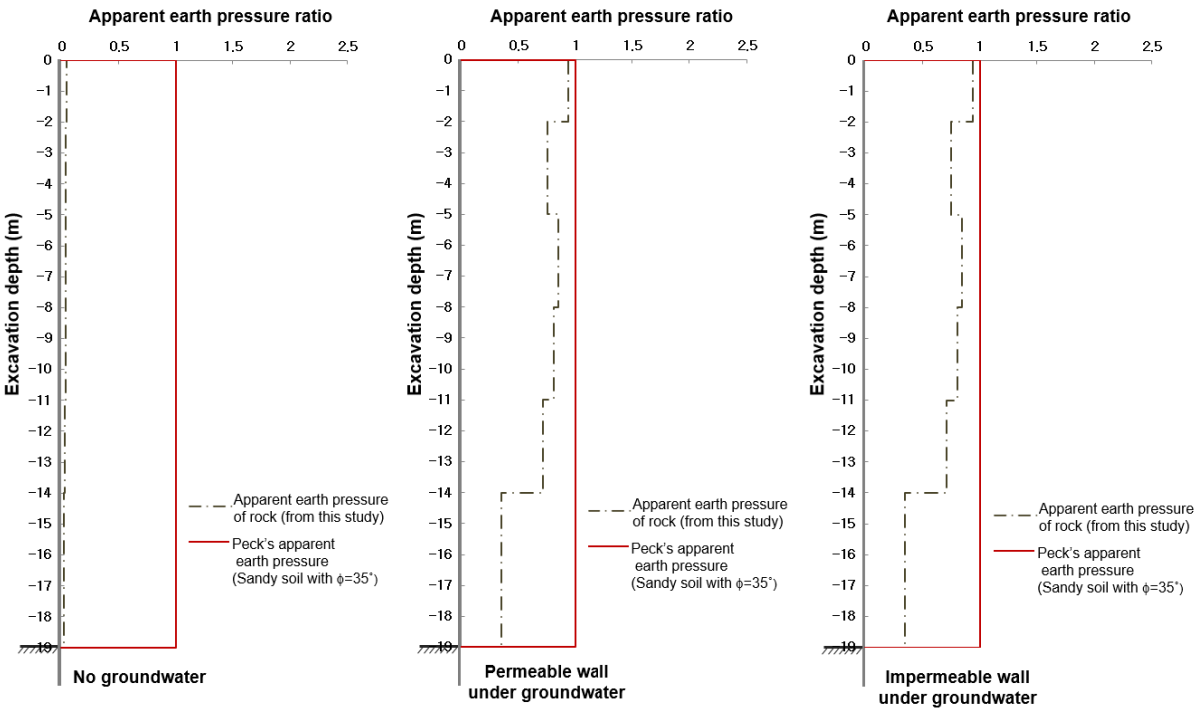

Fig. 8. Comparison of the apparent earth pressures for hard rock (joint inclination angle: 90°)

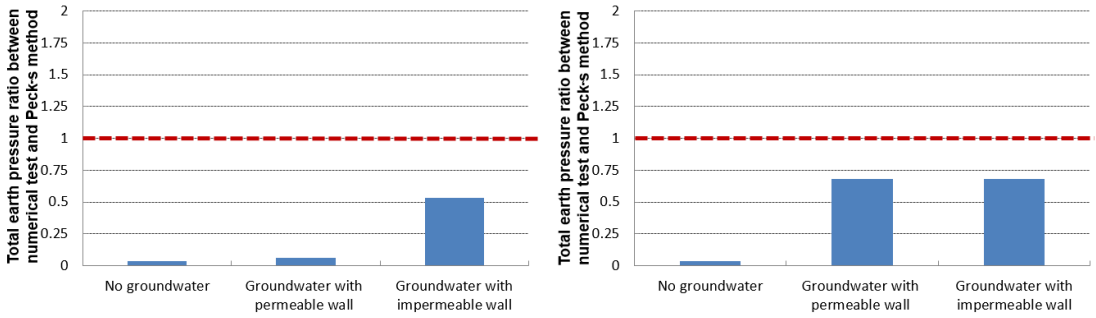

(a) Joint inclination angle: 30° (b) Joint inclination angle: 90°

Fig. 9. Comparison of the total earth pressure ratios between the numerical tests and Peck's empirical method (Hard rock)

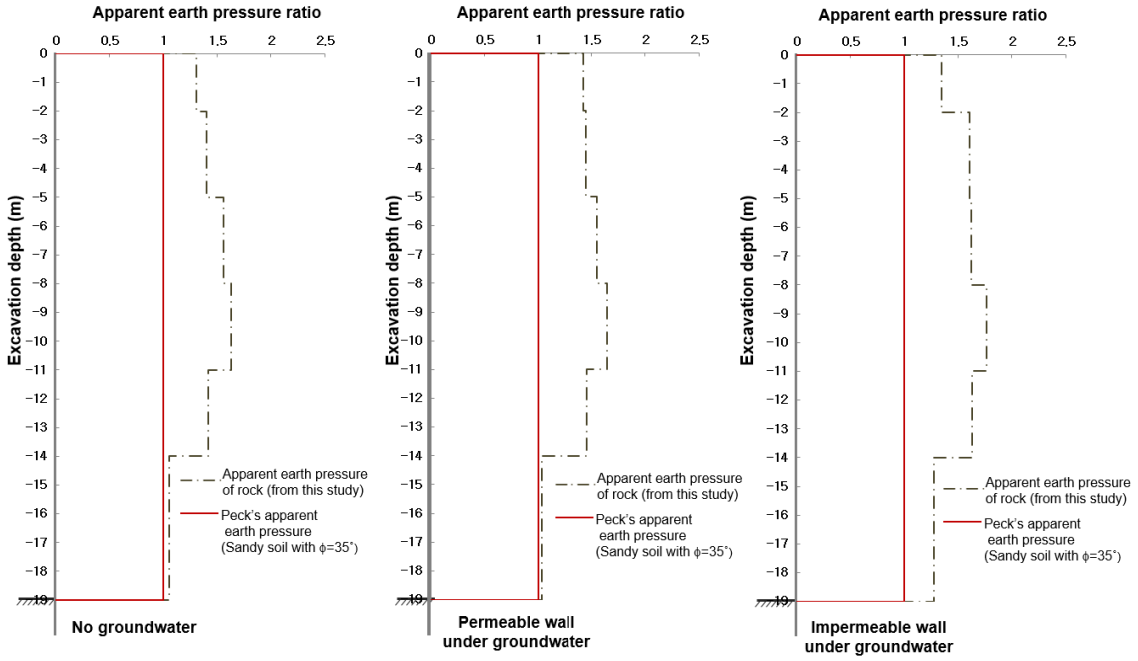

Fig. 10. Comparison of the apparent earth pressures for moderately weathered rock (joint inclination angle: 30°)

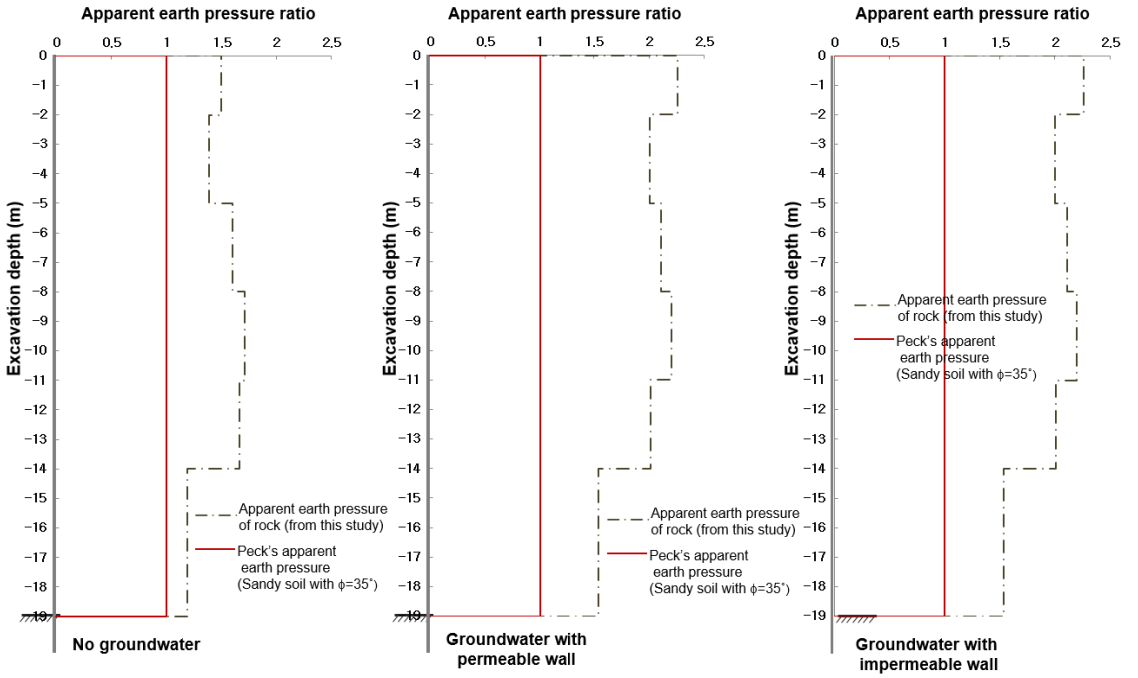

Fig. 11. Comparison of the apparent earth pressures for moderately weathered rock (joint inclination angle: 90°)

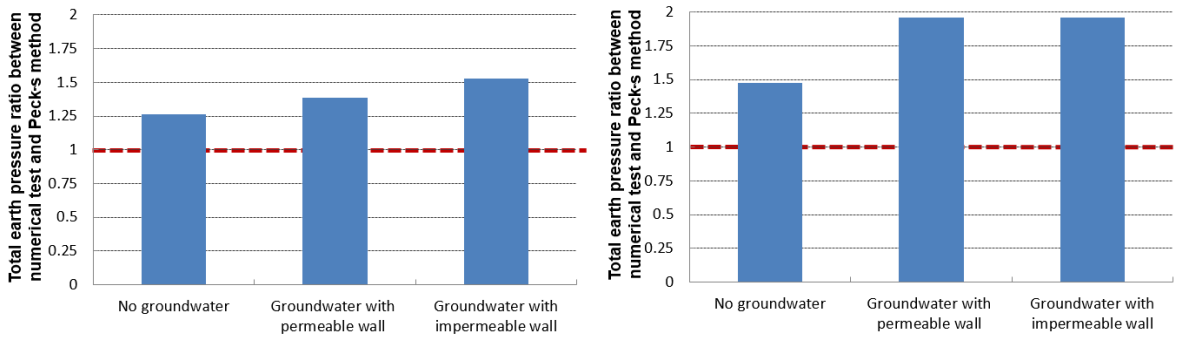

(a) Joint inclination angle: 30°

(b) Joint inclination angle: 90°

Fig. 12. Comparison of the total earth pressure ratios between the numerical tests and Peck's empirical method (Moderately weathered rock)

respectively under different wall permeability and groundwater conditions. In addition, the apparent earth pressures in jointed rock masses were compared with Peck's apparent earth pressure for sand ground with a friction angle of ϕ = 35°. Fig. 12 compares the total earth pressure ratios of the induced earth pressures from numerical analysis with that from Peck's empirical earth pressure for the sand ground.

For a joint inclination angle of 30°, the apparent earth pressures of all the conditions significantly increased compared to those of hard rock condition. The earth pressures of the different wall conditions were not much different (see Figs. 10 and 12) and the total earth pressure ratios between the induced earth pressure and Peck's earth pressure were 1.26, 1.38, and 1.53 for the wall under no groundwater, the permeable wall, and the impermeable wall respectively. The reason can be attributed to the weathered rock condition that increased the earth pressure significantly with weathering itself.

For a joint inclination angle of 90°, the induced apparent earth pressures (see Fig. 11) increased overall when compared with those of the joint inclination angle of 30°. The earth pressure of the permeable wall under groundwater condition was similar to that of the impermeable wall under groundwater condition, which was also observed in the hard rock. The total earth pressure ratios between the induced earth pressure and Peck's earth pressure were 1.48, 1.96, and 1.96 for the wall under no groundwater, the permeable wall, and the impermeable wall respectively.

The study results indicated that as the rock and joint conditions were weathered further, the earth pressure increased, the effect of groundwater decreased, and the effects of joint inclination angles decreased. In addition, the results showed that for better rock and high joint inclination angle conditions, the effects of wall permeability and groundwater were more significant and when the rock was weathered and the joint inclination angle was low, the effects of wall permeability and groundwater on the earth pressure were less significant.

4. Conclusions

The earth pressure on the excavation wall in jointed rock masses was examined. The controlled parameters included wall permeability condition as well as rock type and joint conditions. The following conclusions were drawn:

(1) The earth pressure on an excavation wall in a jointed rock mass are highly affected by the wall permeability condition together with the joint inclination angle and rock type. Besides, the induced earth pressure in a jointed rock mass can be very different from soil ground.

(2) The study clearly showed that the earth pressure can be higher for rock strata than soil ground when the rock and joint characteristics are under unfavorable conditions, such as a weathered joint and rock condition. On the other hand, the earth pressure might be much lower than the soil ground when the rock conditions are favorable.

(3) The results showed that for better rock and high joint inclination angle conditions, the effects of wall permeability and groundwater were more significant and when the rock was weathered and the joint inclination angle was low, the effects of wall permeability and groundwater on the earth pressure were less significant. For hard rock with a joint inclination angle of 30°, the total earth pressure ratios between the induced earth

pressure and Peck's earth pressure were 0.033, 0.06, and 0.53 for the wall under no groundwater, the permeable wall, and the impermeable wall respectively, while the ratios were 0.035, 0.68, and 0.68 respectively for a joint inclination angle of 90°. However, for moderately weathered rock with a joint inclination angle of 30°, the total earth pressure ratios between the induced earth pressure and Peck's earth pressure were 1.26, 1.38, and 1.53 for the wall under no groundwater, the permeable wall, and the impermeable wall respectively, while the ratios were 1.48, 1.96, and 1.96 respectively for a joint inclination angle of 90°.

(4) From the study, it is clear that the wall permeability as well as rock type and joint inclination angle are important parameters influencing the magnitude and distribution of earth pressure, which should be considered when designing the excavation walls in jointed rock mass. In addition, the study results should be limited in the considered conditions and further studies are needed to consider more complex 3D joint structures.

References

1. Bieniawski, Z. T. (1989), *Engineering Rock Mass Classification*, John Wiley & Sons, NY, 272 p.
2. Chae, Y. S. and Moon, I. (1994), Earth pressure on retaining wall by considering local soil condition, Korean Geotechnical Society '94 fall conference paper, pp. 129~138 (in Korean).
3. Goodman R. E. (1989), Introduction to rock mechanics, Wiley & Sons, Yew York, 576 p.
4. Hoek, E. and Brown, E.T. (1988), Underground Excavations in Rock, Institution of Mining and Metallurgy, London, 532 p.
5. Jeong, E. T. and Kim, S. G. (1997), Case study of earth pressure distribution on excavation wall of multi-layered soil, Korean Geotechnical Society '97 spring conference paper, pp. 78~80 (in Korean).
6. Peck, R. B. (1969), Deep excavations and tunneling in soft ground. State-of-the-Art report, Proceedings of the 7th International Conference on Soil Mechanics and Foundation Engineering, Mexico City, State-of-the Art Volume, pp. 225~290.
7. Son, M. (2013), Earth pressure on the support system in jointed rock mass, Canadian Geotech. Journal, Vol. 50, No. 5, pp. 493~502.
8. Son, M. and Adedokun, S. (2015), Effect of support characteristics on the earth pressure in a jointed rock mass, Canadian Geotech. Journal, Vol. 52, pp. 1~12.
9. Son, M., Adedokun, S. and Hwang, Y. (2015), Effect of the earth pressure coefficient on the support system in jointed rock mass, Journal of the Korean-Geoenvironmental Society, Vol. 16, No. 2, pp. 33~43.
10. Son, M. and Park, J. (2014), Physical model test and numerical simulation of excavation wall in jointed rock mass, Canadian Geotech. Journal, Vol. 51, No. 5, pp. 554~569.
11. Son, M. and Yoon, C. (2011), Characteristics of the earth pressure magnitude and distribution in a jointed rockmass, Journal of Korean Society of Civil Engineers, Vol. 31(6), pp. 203~212 (in Korean).
12. Tschebotarioff, G. P. (1973), Foundations, Retaining and Earth Structures, 2nd Ed., MGH.
13. Universal Distinct Element Code, UDEC (2004), User's Manual, Itasca Consulting Group, Inc., Minneapolis, Minnesota, U.S.A.
14. Yoo, C. S. and Kim, Y. J. (2000), Deep excavation in soil, including rock with layers on retaining wall and apparent horizontal displacement of earth pressure, Journal of Korean Geotechnical Society, Vol. 16, No. 4, pp. 43~50 (in Korean).